

L. ZHANG<sup>\*,#</sup>, G. ZHAO<sup>\*</sup>, H. LIU<sup>\*</sup>, G. MIN<sup>\*</sup>, H. YU<sup>\*</sup>

## TUNING THE CRYSTALLOGRAPHIC STRUCTURE AND MORPHOLOGY OF NANOCRYSTALLINE CaB<sub>6</sub> FILMS DEPOSITED BY DC MAGNETRON SPUTTERING

### OPTYMALIZACJA STRUKTURY KRYSZALOGRAFICZNEJ I MORFOLOGII NANOKRYSTALICZNYCH WARSTW CaB<sub>6</sub> NANIESIONYCH METODĄ NAPYLANIA MAGNETRONOWEGO

Through changing the argon pressure, CaB<sub>6</sub> films with different crystallographic orientation and morphology on glass substrates were prepared by direct current (DC) magnetron sputtering method. The film textures, crystallite sizes, composition and morphology were investigated by a spectrum of characterizing techniques in terms of X-ray diffraction (XRD), field emission scanning electron microscopy with energy dispersive spectrometer (FESEM-EDS), atomic force microscopy (AFM), Raman shift spectroscopy. The influence of argon pressure on microstructure was studied. The average grain size increased with the argon pressure increasing from 0.8 Pa to 1.5 Pa. Meanwhile, the dominant crystal face changed from (110) to (100). Then the grain size decreased when the argon pressure increased to 2.0 Pa. The surface morphology evolved from typical cauliflower-like nanocrystalline clusters to faceted rectangular pyramids. It was found that considerable amount of argon atoms were trapped in the films. The formation process of CaB<sub>6</sub> films was also analyzed in this paper.

*Keywords:* CaB<sub>6</sub> films, crystallographic structure, morphology, argon pressure

Warstwy CaB<sub>6</sub> naniesiono na podłoża szkliste metodą magnetronowego rozpylania stałoprądowego (DC). Poprzez kontrolę ciśnienia argonu otrzymano warstwy o różnej morfologii i orientacji krystalograficznej. Strukturę, wielkość krystalitów oraz skład chemiczny warstw badano przy zastosowaniu następujących technik: dyfrakcji rentgenowskiej (XRD), skaningowej mikroskopii elektronowej w połączeniu ze spektroskopią dyspersji energii promieniowania rentgenowskiego (SEM-EDS), mikroskopii sił atomowych (AFM) oraz spektroskopii Ramana. Badano wpływ ciśnienia argonu na mikrostrukturę warstwy. Wraz ze wzrostem ciśnienia argonu z 0,8 Pa do 1,5 Pa zwiększyła się średnia wielkość ziaren przy jednoczesnej zmianie głównych kierunków krystalograficznych – z (110) w (100). Natomiast w wyniku dalszego wzrostu ciśnienia do 2,0 Pa, wielkość ziaren zmniejszyła się. Zaobserwowano także zmiany w morfologii powierzchni. Stwierdzono, że znaczna ilość atomów argonu została uwięziona w warstwach. W niniejszej pracy poddano także analizie proces powstawania warstw CaB<sub>6</sub>.

## 1. Introduction

To explore the unexpected ferromagnetism reported in the slightly doped alkaline-earth metal hexaborides, particularly in CaB<sub>6</sub>, considerable experiments and theory calculation had been done for many years [1-4]. Currently one possible interpretation of the magnetic mechanism is that it maybe originated from intrinsic defects. Considering that thin films usually consist of nanocrystalline or incomplete crystalline structure, which has many grain boundaries and defects, the role of defects in films may be enhanced. Therefore, relevant research focusing on magnetism of thin films was urgently demanded. Coey [5] and Miyazaki [2] reported the pulsed-laser method and RF-magnetron sputtering method respectively which were used to fabricate hexaboride films. Shang [6] investigated the growth condition for alkaline-earth metal hexaboride films by calculating the P-T phase diagrams of the B-metal systems

using the calculation of phase diagram (CALPHAD) technique. Even though, literatures about fabrication method and detailed characterization of hexaboride films were still scarce. Magnetron sputtering is the most widely used method due to its high deposition rate, low sputtering gas pressure, simple structure, low requirements and simple operation. And it is well known that the sputtering gas pressure is one of the most crucial parameters which perform decisive effect on the structure and morphology of deposited films. In this work, CaB<sub>6</sub> films with different crystalline structure and morphology were deposited by tuning the argon pressure. Detailed characterization and mechanism were explored. It's aimed to provide sufficient structure analysis for the following work focusing on building the relationship between structure and magnetic property. Furthermore, the results of this study can be of importance and conducive to the preparation of other alkaline-earth metal hexaboride films.

\* SCHOOL OF MATERIALS SCIENCE AND ENGINEERING, SHANDONG UNIVERSITY, JINAN, CHINA

# Corresponding author: zhanglin2007@sdu.edu.cn

## 2. Experiments

### 2.1. Preparation of films

CaB<sub>6</sub> films were deposited using a direct current magnetron sputtering system (FJL560C3, Shenyang Scientific Instruments Research Institute, China). The sputtering target which was sintered using self-made CaB<sub>6</sub> micron powders in our laboratory [7] was a 60 mm diameter, 5 mm thickness disk. A continually variable DC power supply of 320 V and 0.28 A was used as the power source for sputtering. The negative bias voltage (-100V) was applied to the substrate without intentional heating. The base pressure was lower than  $6 \times 10^{-4}$  Pa. The sputtering gas was argon of 99.9999% purity. Films were deposited under various argon pressures ranging from 0.8, 1.0, 1.5 to 2.0 Pa. The flow rate of argon gas was controlled using mass flow controllers, which was kept constant at 25 sccm. The argon pressure was controlled by manipulating the hand-operated slide valve to control the valve throttle area of the pipeline leading to the turbo molecular pump. The deposition time of 2 h was chosen to achieve a film thickness close to 2.2  $\mu\text{m}$ , which depended on the applied argon pressure. The substrates were 20×30 mm<sup>2</sup> glass and were ultra-sonically pre-cleaned in acetone and ethanol. The target was pre-sputtered for about 15 min to remove impurities.

### 2.2. Characterization

The crystalline structure was examined by X-ray diffraction measurement (Rigaku, Japan) with Cu K $\alpha$  radiation in  $\theta$ -2 $\theta$  mode (40 kV/200 mA). The surface morphology was investigated by an atomic force microscope system in scanning probe microscopy (Dimension Icon, Bruker) and FESEM system (Su-70 Hitachi, Japan), respectively. The chemical composition was analyzed by EDS attachment equipped by the FESEM system. Raman spectra were measured on the Raman spectrophotometer (LABRAM-HR800).

## 3. Results and discussion

### 3.1. Structure

Fig. 1 shows the XRD patterns of CaB<sub>6</sub> films deposited under different argon pressure ranging from 0.8 Pa to 2.0 Pa. It's notable that 0.8 Pa was the lowest argon pressure which could maintain a stable discharge needed for sputtering. For

films deposited under low argon pressure (0.8 or 1.0 Pa), the XRD pattern shows a broad and low peak feature, which is due to the incomplete crystalline and even amorphous structure. While under high argon pressure, peaks change to sharp and high. In the films deposited with the applied argon pressure 1.5 Pa, the intensity of (100) and (200) peaks perform several times than other diffraction peaks. In other words, with the increase of the argon pressure, the crystallization degree of the films increased firstly and then decreased, which reached to a peak level in the films deposited at 1.5 Pa. The peak intensity, FWHM value and grain size estimated by the Scherrer's formula were revealed in TABLE 1 proved the conclusion above.

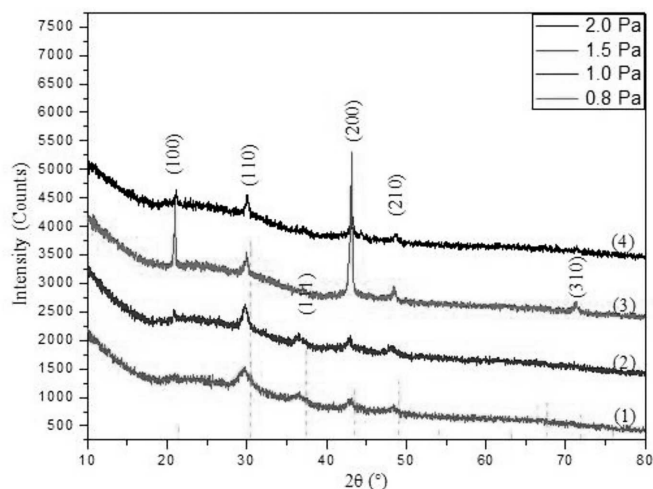


Fig. 1. XRD patterns of CaB<sub>6</sub> films deposited at different argon pressure. (1) 0.8 Pa, (2) 1.0 Pa, (3) 1.5 Pa, (4) 2.0 Pa. The dotted lines indicate peak positions of bulk CaB<sub>6</sub>.

The Raman analysis confirmed the varying crystallization quality of CaB<sub>6</sub> films depended on argon pressure. As shown in Fig. 2. Raman spectra of the as-prepared CaB<sub>6</sub> films compose of three peaks representing the Raman active modes T<sub>2g</sub>, E<sub>g</sub> and A<sub>1g</sub> for CaB<sub>6</sub>, and those peaks are in agreement with other literature [8]. All the peak position information of the films coupled with value of micron powder list in TABLE 2. What's notable is that compared with the peak position of the micron powder, the value of films all shift to the red region. The film deposited at 1.5 Pa shows the largest peak position 768.10, 1127.84 and 1267.97 cm<sup>-1</sup>, respectively. It's obvious that other films deposited with the applied argon pressure over

TABLE 1

A series of XRD data of CaB<sub>6</sub> films for various argon pressures

Argon pressure (Pa)	(100)				(110)				(200)			
	d(A)	I%	FWHM	GS(A)	d(A)	I%	FWHM	GS(A)	d(A)	I%	FWHM	GS(A)
0.8					3.0057	100.0	0.827	100	2.1048	57.8	0.662	130
1.0	4.2500	38.6	0.394	212	2.9969	100.0	0.683	122	2.1080	49.6	0.579	150
<b>1.5</b>	<b>4.2342</b>	<b>40.4</b>	<b>0.276</b>	<b>313</b>	<b>2.9789</b>	<b>14.7</b>	<b>0.478</b>	<b>176</b>	<b>2.0958</b>	<b>100.0</b>	<b>0.356</b>	<b>250</b>
2.0	4.1998	62.7	0.344	245	2.9723	97.1	0.465	181	2.0902	100.0	0.408	216

\* GS means the grain size estimated using the Scherrer's formula

or below 1.5 Pa could lead the peak position to become down-shift and broadening. H. Richter et al [9] presumed that down-shift and broadening of the peak position was attributed to a nanocrystalline or incomplete crystalline structure. In a word, the crystalline degree obtained from the Raman spectra in this work was consistent with those from XRD characterization.

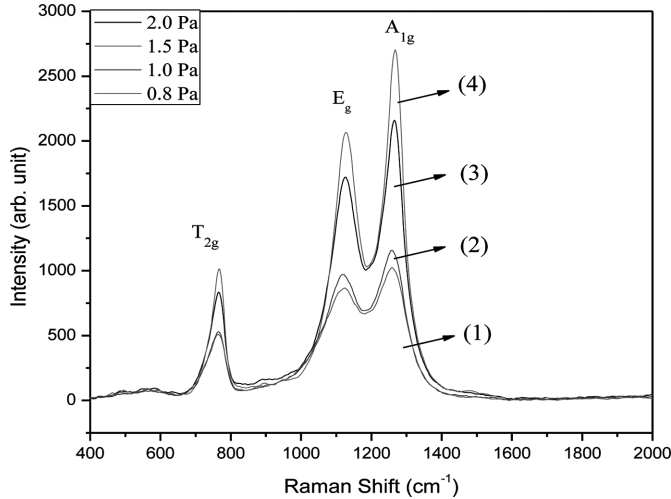


Fig. 2. Raman spectra of  $\text{CaB}_6$  films deposited with different applied argon pressure. (1) 0.8 Pa, (2) 1.0 Pa, (3) 1.5 Pa, (4) 2.0 Pa

TABLE 2  
Values of Raman scattering peaks for different  $\text{CaB}_6$  films and powder

$\text{CaB}_6$ specimen		$T_{2g}(\text{cm}^{-1})$	$E_g(\text{cm}^{-1})$	$A_{1g}(\text{cm}^{-1})$
films	0.8 Pa	763.92	1123.66	1259.60
	1.0 Pa	763.00	1119.48	1257.52
	<b>1.5 Pa</b>	<b>768.10</b>	<b>1127.84</b>	<b>1267.97</b>
	2.0 Pa	766.00	1125.75	1265.88
micron powder *		780.10	1141.00	1283.50

\* The powder that used to sinter the target for sputtering [7]

Considering that films were deposited under negative substrate bias voltage (-100V), it may be the ion bombardment that leading to the changing trend of crystallization. It's known that the bombardment caused by the applied bias voltage could provide additional energy to the condensed particle. Danson et al. [10] reported that this kind of bombardment corresponding to elevate substrate temperature could improve crystallization. With the argon concentration increasing, there will be more  $\text{Ar}^+$  reached the substrate, the ion bombardment was exaggerated. It can illustrate the phenomenon that the crystallization degree increased with the argon pressure changing from 0.8 Pa to 1.5 Pa in this paper. As for the weak decreasing of grain size with the argon pressure increasing from 1.5 Pa to 2.0 Pa, it may be caused by the argon atoms scattering to the sputtered atoms intensified by high argon concentration. This collision between argon and the sputtered atoms could decrease the condensing particles' kinetic energies before they reached the substrate. Thus the following diffusion and thermal movement could be limited, which was not beneficial to the crystallization.

TABLE 3  
Comparison of different element amount in different films deposited at 0.8 Pa and 2.0 Pa obtained by EDS

Element	Atomic% P(Ar)/2.0 Pa	Atomic% P(Ar)/0.8 Pa
B K	79.58	84.93
O K	10.95	2.37
Ar K	0.10	1.27
Ca K	9.37	11.43

What's interesting, there was considerable amount of argon atoms trapped into the film. And it is shown in TABLE 3. As the applied argon pressure increased from 0.8 Pa to 2.0 Pa, the ratio of Ca to Ar changed from 0.1 to 0.01. Considering that the poorly crystallized thin film deposited at 0.8 Pa a performed complex structure with a great number of grain boundaries and defects, the trapped Ar exist in the location of the grain boundaries and defects rather than replaced the Ca or B in the crystalline lattice. And the trapped Ar may hinder the film to form perfect crystalline structure to some extent. Because of the sensitivity of light elements of EDS technology, the results also revealed that the atomic ratio of B to Ca was about 8:1, which was larger than the stoichiometric ratio of 6:1.

In addition, the crystal orientation of thin films was investigated and the results demonstrated that the preferred orientation of grains was effectively affected by argon pressure. As shown in Fig. 1, thin films deposited at low pressure had the same dominant diffraction peak (110) compared with the bulk  $\text{CaB}_6$ . The observed intensity ratio of different peaks was also coupled well with those in bulk  $\text{CaB}_6$ , which indicated a nanocrystalline multiphase structure. On the other hand, thin films deposited at high pressure had a strong (100) and (200) peaks, which means the films were textured along the (100) orientations. A pronounced (100) texture and a weak one to an almost random orientation of the  $\text{CaB}_6$  phase were observed in the films deposited at 1.5 Pa and 2.0 Pa, respectively.

The structure evolution of different argon pressure can be attributed to the shadowing effect and different surface mobility of adatoms on different crystal orientations [11]. Karabacak [12] assumed that low surface mobility islands preferred to develop along the directions perpendicular to the film, while the higher surface mobility islands preferred lateral islands growth. Because of the fast growth of the low surface mobility islands in the vertical directions, the shadowing effect enhanced its growth, at the same time suppressed the higher surface mobility islands' lateral growth, and consequently making the vertical growth grains to be the dominant ones. In this paper, as the argon pressure increased to a high value, the shadowing effect and crystal growth on low mobility crystal orientations were enhanced, which led the dominant crystalline face change from the thermodynamically favorable (110) to the (100) of low mobility.

### 3.2. Morphology

Fig. 3 shows the dependence of the AFM surface morphologies of films on applied argon pressure. It can be clearly seen that the value of root mean square (Rms) roughness

increased from about 23.1 to 61.4 nm with the increasing argon pressure from 0.8 to 1.5 Pa, and then decreased to 50.1 nm when the argon pressure reached to 2.0 Pa as shown. What's notable, the morphology of the films evolved from a cauliflower-like structure composed with nanocrystalline cluster to faceted shape with the argon pressure increasing among the range investigated in this work. The variety of the Rms could be attributed to the different grain size and shape. There is no doubt that the larger grain size and the shape faceted morphology could lead to a high value of Rms.

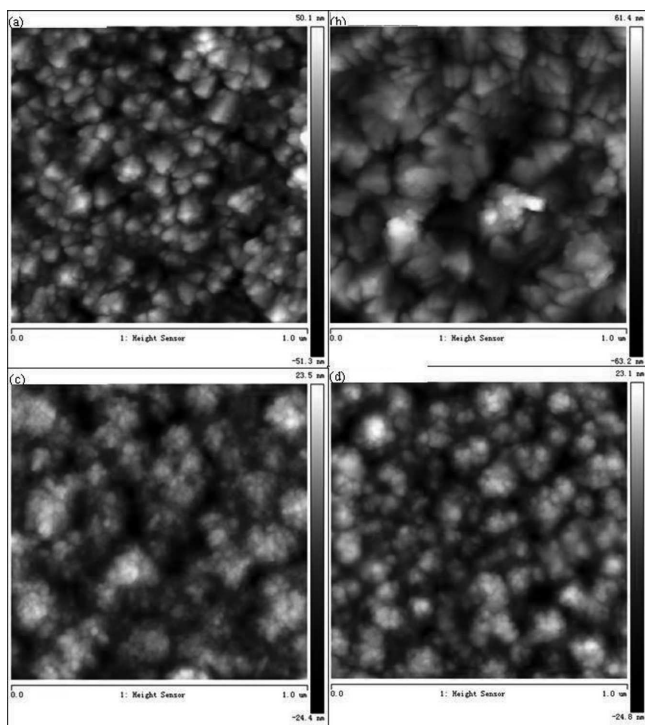


Fig. 3. AFM micrographs of  $\text{CaB}_6$  films deposited at various argon pressure. (a) 2.0 Pa, (b) 1.5 Pa, (c) 1.0 Pa, (d) 0.8 Pa

To understand the formation and the mechanism of different topology, detailed argon pressure-dependent evolution of morphology were studied. In Fig. 4, a sequences of high-magnification SEM images reveals the detailed feature of the top surface and the cross section of the films respectively. For the film deposited at lower argon pressure, as shown in Fig. 4(c), the commonly observed cauliflower-like morphology with smoother, denser, and random directional protrusions, was attributed to the fine-grained and maybe even incomplete crystalline structure. As applied argon pressure increased to a high value, here was 1.5 or 2.0 Pa, the top view showed a faceted topology covered mainly by typical pyramidal shaped facet, and even some ridge-like facets were observed in films deposited at 2.0 Pa especially. The morphology characterized by FESEM was agree well with the result of AFM as depicted above. Integrating the typical morphology and the crystalline orientation analysis, it's not difficult to presume that the fourfold symmetric (110) pyramid-shaped facets and twofold symmetric (110) ridge-like facets are all the top of the (100) orientated columnar crystalline, which grow along the direction perpendicular to the surface of the films. This structure is as similar as the cubic  $\beta$ -phase W (100) nanorods with a pyramidal tip having four (110) facets, which reported

by Karabacak et al [12]. It is clearly shown in Fig. 4, and the insets in Fig. 4 (a), (b) are schematic ridged and pyramidal shape, respectively.

The mechanism for the dependence of morphology on argon pressure was studied. It's well known that the morphology could be determined by the crystalline structure. Considering the relationship between the crystalline orientation and the argon pressure discussed above, it's the enhanced shadowing effect with the increasing argon pressure and the different surface mobility of adatoms on different crystal face that co-affected the morphology. High argon concentration reduces the directionality of the incoming sputtering atoms to the substrate and hence enhances the shadowing effect. What's more, shadowing effect is responsible for the formation of a columnar structure [13] and the enhanced shadowing effect with the increasing argon pressure could also be proved by the fact that the cross section view of the films changed from the loose coarse structure to the dense fine columnar structure as shown in Fig. 4(a')-(c').

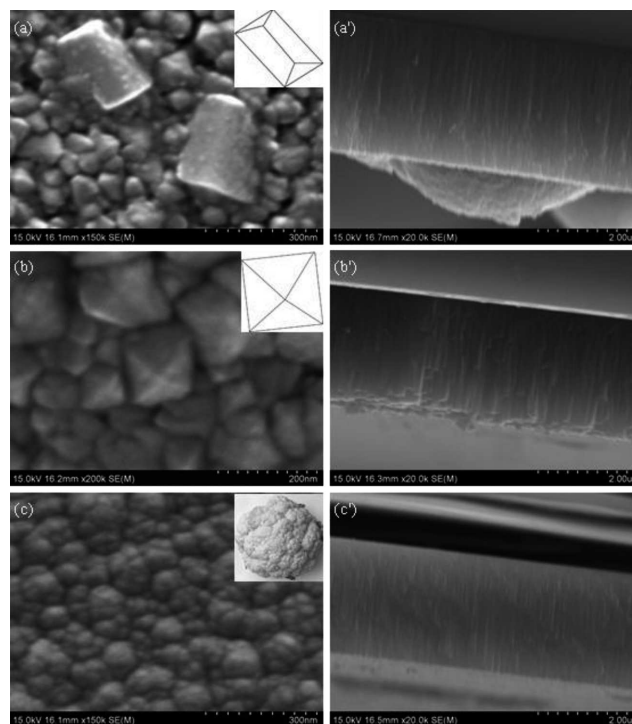


Fig. 4. SEM surface images (a)-(c) and cross-section images (a')-(c') of  $\text{CaB}_6$  films deposited at different argon pressure: (a), (a') 2.0 Pa, (b), (b') 1.5 Pa, (c), (c') 0.8 Pa

#### 4. Conclusion

The present work investigated the effect of argon pressure on grain size, orientation and morphological properties of  $\text{CaB}_6$  films deposited by dc-magnetron sputtering. The main result of this investigation are as follows: (1) the grain size increased with the argon pressure increased from 0.8 Pa to 1.5 Pa, then performed a slightly decreasing trend; (2) as the argon pressure increased, the crystalline structure changed from a non-directional structure to an textured one with preferred (100) plane; (3) the surface morphology of the films varying from commonly observed cauliflower-like morphology to well faceted one with the increasing argon pressure.

It's presumed that the crystalline structure evolution is co-affected by shadowing effect and different surface mobility of adatoms on different crystal orientations. Within the range of the argon pressure investigated, it's the enhanced shadowing effect and crystal growth on low mobility orientations at high pressure that lead to the change of dominant crystalline plane from thermodynamically favorable (110) to (100). The (100) plane is bounded and tipped by (110) facets to obtain the final thermodynamic equilibrium state. Thus, the commonly observed structure at high pressure is the (100) orientated columnar crystalline tipped by fourfold symmetric (110) pyramid-shaped facets or twofold symmetric (110) ridge-like facets. And it's obvious that the morphology is determined by the crystalline structure. It's demonstrated that the structural and morphological properties of CaB<sub>6</sub> films grown under the conditions investigated can be tuned by controlling the argon pressure.

#### Acknowledgements

The authors wish to acknowledge the financial support from National Natural Science Foundation of China (NSFC, No. 51102154).

#### REFERENCES

- [1] D.P. Young, D. Hall, M.E. Torelli, Z. Fisk, J.L. Sarrao, J.D. Thompson, H.R. Ott, S.B. Oseroff, R.G. Goodrich, R. Zysler, *Nature* **397**, 412 (1999).
- [2] Y. Sakuraba, H. Kato, F. Sato, T. Miyazaki, *Phys. Rev. B* **69**, 140406 (2004).
- [3] S.E. Lofland, B. Seaman, K.V. Ramanujachary, Nanjing Hur, S.W. Cheong, *Phys. Rev. B* **67**, 020410 (2003).
- [4] R. Monnier, B. Delley, *Phys. Rev. Lett.* **87**, 157204 (2001).
- [5] L.S. Dorneles, M. Venkatesan, M. Moliner, J.G. Lunney, and J.M.D. Coey, *Appl. Phys. Lett.* **85**, 6377 (2004).
- [6] S. Shang, Z.K. Liu, *Appl. Phys. Lett.* **90**, 091914 (2007).
- [7] L. Zhang, G.H. Min, H.S.H. Yu, *Ceram. Int.* **35**, 3533 (2009).
- [8] N. Ogita, S. Nagai, N. Okamoto, F. Iga, S. Kunii, J. Akimitsu, M. Udagawa, *Physica B* **68**, 224305 (2003).
- [9] H. Richter, Z.P. Wang, L. Ley, *Solid State Commun.* **39**, 625 (1981).
- [10] N. Danson, I. Safi, G.W. Hall, R.P. Howson, *Surf. Coat. Technol.* **99**, 147 (1998).
- [11] Arif S. Alagoz, in: J. Lou (Ed.), *MRS Proceedings 1224*, Boston (2009).
- [12] T. Karabacak, A. Mallikarjunan, J. P. Singh, D. Ye, G.-C. Wang, T.-M. Lu, *Appl. Phys. Lett.* **83**, 3096 (2003).
- [13] R. Messier, A.P. Giri, R.A. Roy, *J. Vac. Sci. Technol. A* **2**, 500 (1984).